Helical Structures of Tilted Chiral Lipid Bilayers Viewed as Cholesteric Liquid Crystals

Ou-Yang Zhong-can
Chinese Center of Advanced Science and Technology (World Laboratory), P.O. Box 8730 and Institute of Theoretical Physics, P.O. Box 2735, Beijing, China

Liu Ji-xing
Institute of Theoretical Physics, P.O. Box 2735, Beijing, China
(Received 3 May 1990)

We have derived the tilt and surface shape-equilibrium equations for tilted chiral lipid bilayers (TCLB) in analogy with cholesteric liquid crystals. On a cylindrical surface the field of tilt directions of TCLB molecules forms a right-handed helix with 45° gradient angle for $k_2 > 0$ or a left-handed helix with $-45°$ for $k_2 < 0$, where k_2 is the cholesteric chiral curvature modulus. In addition, there exists another type of helical structure which looks like twisted strips or helicoids. We also show that on a spherical surface the tilt field has at least two singular points. These results explain the observed succession of transitions from a vesicular dispersion to a phase involving helical structures and then to tubes.

PACS numbers: 82.70.−y, 02.40.+m, 61.30.Gd

Several recent papers have reported helical structures of various amphiphiles,[1-7] especially lecithin,[5-7] as they are precipitated from water solutions or solutions with organic solvents, or as they are obtained from the freezing of fluid bilayers. One type of the helical structure looks like a ribbon wound on a cylinder with spiral gaps. Sometimes the gap closes as time goes on, so that the ribbon transforms into a prolate tube. Some of the tubes are multilamellar and look like a soda straw (Fig. 3 of Ref. 5). A remarkable property of the observed helical structure is that the spiral makes an angle of nearly 45° with the tube axis.[4] Another type of helical structure is a helicoid or twisted strip. The twisted strip seems to be a crossover from the vesicular dispersion to the helical structure of the first type (Figs. 1A–1D of Ref. 1) or a crossover region of a bending wound-ribbon helix (Fig. 1B of Ref. 2). Technically, these structures can be used in making electro-optical elements, microelectronic elements, reagent delivery vehicles, and microsurgical materials.[8] A recent significant advance is the successful coating of the tubes with nickel and/or copper to make them highly conductive.[9]

On the theoretical side, a major challenge is to understand the mechanism of the winding and the twisting of the lipid bilayers. Assuming competition between the spontaneous torsion of the edge and the bending of the bilayer, Helfrich[10] developed a theoretical treatment of the wound-ribbon helices. The tube formation was explained by de Gennes[11] in terms of a buckling of the flat solid ribbon due to the ferroelectric polarization charges on its edges. More recently, Helfrich and Prost[12] proposed an improved theory that employs a new linear term of C_2 or D_2 symmetry linked to the molecular chirality in the bending energy of bilayers. However, all these theories give no discussion of the more difficult cases of the twisted strips and the vesicular dispersion.

Our approach follows Helfrich and Prost[12] in dealing with the membrane elasticity, but, instead of using a term of C_2 or D_2 symmetry, we introduce a linear term with D_∞ symmetry to study helical-structure problems. In other words, instead of considering ferroelectric and chiral smectics (S_c^*), we consider cholesterics. With this improvement of the symmetry, we are now able to deal not only with wound-ribbon helices but also with twisted strips and vesicles of tilted chiral lipid bilayers (TCLB). Based upon the curvature-elasticity model of cholesterics, we find the general tilt equation and surface-equilibrium equation of the TCLB. By solving these equations we can show that, on a cylinder, the tilt-direction field of TCLB molecules forms right-handed helices with 45° gradient angle for $k_2 > 0$ and left-handed helices with $-45°$ gradient angle for $k_2 < 0$, where k_2 is the chiral curvature modulus of the cholesteric liquid crystals. In particular, we can show that the pitches of the helices are of the order of that of cholesterics (0.1–10^2 μm). The twisted-strip solution and the tilt field of spherical vesicles are also obtained. For spherical vesicles we find that the field has more than two singular points. Our calculation also indicates a decreasing sequence of the elastic energies associated with vesicle, twisted-strip, and wound-ribbon solutions. This result explains the experimentally observed sequence of transitions from the vesicular dispersion to the twisted-strip helix and finally to the wound ribbon.

The bulk elastic free-energy density of a cholesteric liquid crystal may be written[13] (neglecting a trivial constant),

$$g_{\mathrm{LC}} = \tfrac{1}{2}[k_{11}(\nabla\cdot\mathbf{d})^2 + k_{22}(\mathbf{d}\cdot\nabla\times\mathbf{d})^2 + k_{33}(\mathbf{d}\cdot\nabla\mathbf{d})^2] - k_2\mathbf{d}\cdot\nabla\times\mathbf{d}, \quad (1)$$

where $\mathbf{d}$ is the director field and k_{11}, k_{22}, and k_{33} are the splay, twist, and bend elastic moduli and the last term characterizes the chirality of the cholesteric liquid crys-

tal. All observations demonstrate that the chirality of the molecules plays a crucial role in the formation of the helical structures of TCLB. Here, for simplicity, we consider for the moment only the last term of Eq. (1):

$$g_{\mathrm{ch}} = -k_2 \mathbf{d}\cdot\nabla\times\mathbf{d}\,. \tag{2}$$

In other words, we consider a TCLB with strong chirality. We may consider the TCLB as a curved cholesteric layer sandwiched between two surfaces $\mathbf{Y}(u,v)$ and $\mathbf{Y}(u,v)+\mathbf{n}(u,v)t$, where $\mathbf{n}$ is the unit normal of the surface $\mathbf{Y}$ and t is the thickness of the TCLB.

Since t is much smaller than the linear dimension of the surface, we may calculate the elastic energy of the TCLB as

$$F=\int g_{\mathrm{ch}}\,dV = t\oint g_{\mathrm{ch}}\,dA\,, \tag{3}$$

where dV is the volume element of the bulk and dA is the area element of the surface $\mathbf{Y}$. Let us represent the tilt vector field by

$$\mathbf{d}=d_1\mathbf{Y}_1+d_2\mathbf{Y}_2+\mathbf{n}\cos\theta_0\,, \tag{4}$$

where $\mathbf{Y}_1=\partial_\mu\mathbf{Y}$, $\mathbf{Y}_2=\partial_v\mathbf{Y}$, the scalar fields d_1 and d_2 associated with $\mathbf{Y}_1$ and $\mathbf{Y}_2$ describe the tilt-direction field on the surface, and θ_0 is the angle between the director (the average direction of the hydrocarbon chain of the TCLB molecules) and the surface normal $\mathbf{n}$. In general, for the $L_{\beta*}$ phase of a TCLB, θ_0 is assumed to be constant. From Eqs. (2) and (3) we have the elastic energy per unit area:[14]

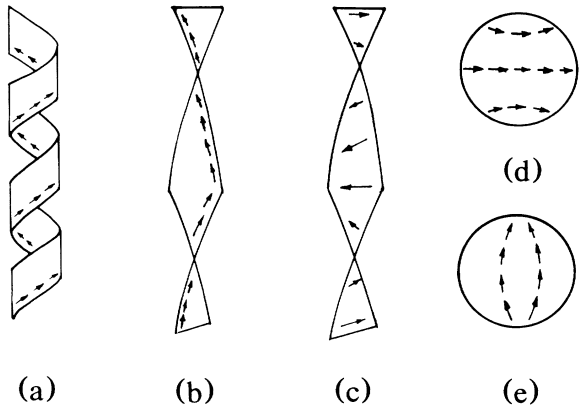

FIG. 1. Schematic illustrations of the helical structures: (a) wound ribbon; (b),(c) the twist strips; (d),(e) spherical vesicles. The arrows represent the local tilt direction.

$$G=tg_{\mathrm{ch}}=k_2 t\epsilon_{3\lambda j}[g_{ik}(d_{k,j}+\Gamma^k_{jl}d_l)\cos\theta_0-2L_{jk}g_{il}d_k d_l]g^{-1/2}\,. \tag{5}$$

Here, ϵ_{ijk} is the permutation tensor, g_{ij} and L_{ij} are the first and second fundamental forms of the surface, respectively, $g=\det(g_{ij})$, and Γ^k_{ij} is the Christoffel symbol.

The Euler-Lagrange equations for G give the tilt-equilibrium equation

$$2\lambda g^{1/2}g_{ij}d_j+k_2\epsilon_{3jk}[2(g_{kl}L_{ij}+g_{ik}L_{je})d_l\cos\theta_0-(g_{ij,k}+g_{kl}\Gamma^l_{ij})\cos^2\theta_0]=0\quad(i=1,2)\,, \tag{6}$$

where $\lambda(u,v)$ is the unknown Lagrange multiplier associated with the condition

$$\mathbf{d}\cdot\mathbf{d}=1\,.$$

If the equilibrium surface $\mathbf{Y}$ is given, we can solve Eq. (6) for d_1, d_2, and λ under the condition $\mathbf{d}\cdot\mathbf{d}=1$. However, the search for an equilibrium surface necessitates the calculation of the energy variation with the surface shape $\mathbf{Y}$. The procedure of such a calculation is illustrated in Ref. 15. We do not give details here but write down the condition of equilibrium directly:

$$g^{-1/2}k_2 t\epsilon_{3ji}[(Kg_{jk}-2HL_{jk})+(\partial_j\partial_k+\partial_m\Gamma^m_{jk})]g_{il}d_k d_l\cos\theta_0-2\lambda L_{ij}d_i d_j=0\,, \tag{7}$$

where H and K are the mean curvature and Gaussian curvature, respectively. In fact, Eq. (6) expresses the balance of the force moment, while Eq. (7) gives the balance of the normal forces per unit area of the surface. Both Eqs. (6) and (7) involve the elasticity-induced stresses and torsions of the curvature elasticity.

Application of Eqs. (6) and (7) to the case of a cylindrical surface of radius ρ_0 represented by

$$\mathbf{Y}=(\rho_0\cos\phi,\ \rho_0\sin\phi,\ z) \tag{8}$$

shows that it is an equilibrium surface, provided the tilt field satisfies

$$d_1=2^{-1/2}\rho_0^{-1}\alpha_1\sin\theta_0,\quad d_2=2^{-1/2}\alpha_2\sin\theta_0\,, \tag{9}$$

where $u=\phi$, $v=z$, and $(\alpha_1,\alpha_2)=(\pm1,\pm1)$ or $(\pm1,\mp1)$ depending on the sign of k_2 (see below). Since the tilt on the edges of the wound ribbon should be along the edge lines, Eq. (9) shows that the tilt field and the edge lines are helices around the cylinder with $\pm45°$ (or $\mp135°$) gradient angle [Fig. 1(a)]. This result agrees with the experimental observations.[1-5]

For a helicoidal surface of radius ρ_0 and pitch $2\pi|b|$ [Figs. 1(b) and 1(c)] represented by

$$\mathbf{Y}=(\rho\cos\phi,\ \rho\sin\phi,\ b\phi)\quad(0\le\rho\le\rho_0)\,, \tag{10}$$

Eqs. (6) and (7) show that it is an equilibrium surface if and only if

$$d_1=0,\quad d_2=\alpha_2(\rho^2+b^2)^{-1/2}\sin\theta_0\,, \tag{11}$$

or

$$d_1=\alpha_1\sin\theta_0,\quad d_2=0. \tag{12}$$

Here $u=\rho$, $v=\phi$, and the pair (α_1,α_2) has the same meaning as in the case of the cylindrical surface. The tilt field given by Eq. (11) [Fig. 1(b)] may represent the experimentally observed twisted strip, since it may change into the wound-ribbon helix without changing the local tilt. The tilt is given by Eq. (12) [Fig. 1(c)] has to be ruled out, since the tilt on the edge is perpendicular to the edge line.

On an equilibrium spherical surface of radius r_0, with the same notation as in Ref. 15, both the latitude lines,

$$d_1=0,\quad d_2=\alpha_2 r_0^{-1}\sin\theta_0\sin^{-1}\theta, \tag{13}$$

and the longitude lines,

$$d_1=\alpha_1 r_0^{-1}\sin\theta_0\sin^{-1}\theta,\quad d_2=0, \tag{14}$$

are solutions of Eq. (6) [Figs. 1(d) and 1(e)]. In both solutions the north pole and the south pole are rotational dislocations. This is not surprising, since it is well known in differential geometry that on a topological sphere a line field has at least two singular points. It is these rotational dislocations that give a higher energy to the vesicle conformation and induce the vesicular dispersion, as pointed out by de Gennes.[11] The same geometry, shown in Fig. 1(e), was invoked by de Gennes in explaining the tube formation.

From Eqs. (3), (8), and (9), we have the energy of the wound-ribbon helix as

$$F_W=-2\alpha_1\alpha_2 k_2 A t\rho_0^{-1}\cos\theta_0\sin^2\theta_0, \tag{15}$$

where A is the total area. It is clear that for $k_2>0$ the right-handed helix ($\alpha_1\alpha_2=1$) has a lower energy than the left-handed one ($\alpha_1\alpha_2=-1$) and vice versa for $k_2<0$. This is in agreement with the case of cholesteric liquid crystals. Similarly, we have the energy of the twisted strip F_T as

$$F_T=-2k_2 A t\rho_0^{-1} f(\rho_0/b)\cos\theta_0\sin^2\theta_0, \tag{16}$$

where the factor $f(x)$ is given by

$$f(x)=2x\ln\left[x+\frac{(1+x^2)^{1/2}}{x(1+x^2)^{1/2}+\ln[x+(1+x^2)^{1/2}]}\right]. \tag{17}$$

Numerical analysis shows that

$$|f(x)|\le 0.984. \tag{18}$$

Thus, F_T is always greater than F_W. In the case of the sphere we have, for both geometries, the energy

$$F_S=0. \tag{19}$$

The result that $F_W<F_T<F_S$ confirms the observed transitions[1] from vesicular dispersion to twisted strip and wound ribbon.

The above-mentioned results seem to agree satisfactorily with many experimental observations. However, there is still the problem of the size of the helical structures. In order to show the general behavior, we consider the simplified case of one elastic constant, i.e., $k_{11}=k_{22}=k_{33}=k$. In this case Eq. (1) simplifies to

$$g_{LC}=g_{NL}+g_{ch},$$

where

$$g_{NL}=(k/2)[(\nabla\cdot\mathbf{d})^2+(\nabla\times\mathbf{d})^2]. \tag{20}$$

Now, we have for the wound ribbon

$$F_{NL}=\int g_{NL}\,dV=ktA(1+\sin^2\theta_0)/2\rho_0^2. \tag{21}$$

The total elastic energy F_{WT} becomes

$$F_{WT}=F_{NL}+F_W$$

$$=At[k(1+\sin^2\theta_0)/2\rho_0^2-2|k_2|\cos\theta_0\sin^2\theta_0/\rho_0]. \tag{22}$$

Minimization of F_{WT} with respect to ρ_0 yields

$$\rho_0=(k/2|k_2|)(1+\sin^2\theta_0)/(\sin\theta_0\cos^2\theta_0). \tag{23}$$

The ratio $k/|k_2|$ is simply the pitch p_{ch} of the cholesteric liquid crystal divided by π.[16] Since the gradient angle of the ribbon helix is equal to $\pm 45°$, we find that the pitch of the helix p is

$$p=2\pi\rho_0=p_{ch}(1+\sin^2\theta_0)\sin^{-1}\theta_0\sin^{-1}2\theta_0. \tag{24}$$

The pitch p_{ch} of cholesterics is of the order of 0.1–10^2 μm,[16] and therefore, the radius and the pitch of the helices is also of the order of 0.1–10^2 μm. This is in good agreement with the experimental data.[1–7] Equations (22) and (23) indicate that, as the area A increases, the total energy F_{WT} becomes more negative. This may explain the formation of prolate tubes and multilamellar aggregations.

Finally, in order to compare our theory with previous theories, we have used some differential-geometry technology and derived the following general form of the chiral elastic energy (3):

$$F=\int g_{ch}\,dV=-k_2 t\cos\theta_0\oint\mathbf{d}\cdot d\mathbf{l}$$

$$-2k_2\sin^2\theta_0\oint\tau_g\,dA, \tag{25}$$

where the first term is the line integral taken around the edge line of the TCLB, and the second one is the surface integral of the geodesic torsion of the local tilt field. The geodesic torsion τ_g may be written as[17]

$$\tau_g=(c_1-c_2)\sin\varphi\cos\varphi, \tag{26}$$

where c_1 and c_2 are the two principal curvatures and φ is the angle from one principal direction to the local tilt direction. The angular dependence is just what Helfrich

and Prost[12] found in the S_c^* model. There are two terms in our expression of the elastic energy. The one that depends on the surface integral will give the result which is found by Helfrich and Prost. The other one, the line-integral term, does not appear in their work. However, it has some important consequences. For a half of a sphere, as shown in Fig. 1(d), it implies a negative edge energy if k_2 corresponds to the appropriate rotational senses. This explains the aggregation of narrow and prolate ribbon structures, which have obviously longer edge lengths at fixed area than other shapes, e.g., a half of a sphere.

In summary, we have developed a theory of the helical structures of TCLB as cholesteric membranes. Our predictions agree very well with the experimental observations.[1-7] Thus, the known properties of cholesteric liquid crystals may well be useful in understanding these helical structures of TCLB's. For example, the molecular theory of cholesterics may reveal the nature of their formation. Experiments to measure directly the tilt field would be a useful check on our theory.

We are grateful to Professor W. Helfrich for stimulating discussion when this work was begun, and we thank Professor M. Wortis for a critical reading of the manuscript. This work was supported partially by the National Natural Science Foundation of China.

[1]N. Nakashima, S. Asakuma, J.-M. Kim, and T. Kunitake, Chem. Lett. **1984**, 1709.

[2]K. Yamada, H. Ihara, T. Ide, T. Fukuumoto, and C. Hirayama, Chem. Lett. **1984**, 1713.

[3]N. Nakashima, S. Asakuma, and T. Kunitake, J. Am. Chem. Soc. **107**, 509 (1985).

[4]P. Yager and P. Schoen, Mol. Cryst. Liq. Cryst. **106**, 371 (1984).

[5]P. Yager, P. Schoen, C. Davies, R. Price, and A. Singh, Biophys. J. **48**, 899 (1985).

[6]J.-H. Fuhrhop, P. Schneider, E. J. Boekema, and W. Helfrich, J. Am. Chem. Soc. **110**, 2861 (1988).

[7]R. M. Servuss, Chem. Phys. Lipids **46**, 37 (1988).

[8]J. M. Schnur *et al.*, Thin Solid Films **152**, 181 (1987).

[9]J. M. Schnur *et al.*, Invention Disclosure NC 70238 (1986).

[10]W. Helfrich, J. Chem. Phys. **85**, 1085 (1986).

[11]P.-G. de Gennes, C. R. Acad. Sci. Ser. 2, **304**, 259 (1987).

[12]W. Helfrich and J. Prost, Phys. Rev. A **38**, 3065 (1988).

[13]F. C. Frank, Discuss. Faraday Soc. **25**, 19 (1958).

[14]The details appear in a full paper by the present authors which will be published elsewhere.

[15]Ou-Yang Zhong-can and W. Helfrich, Phys. Rev. A **39**, 5280 (1989).

[16]P.-G. de Gennes, *The Physics of Liquid Crystals* (Clarendon, Oxford, 1974).

[17]M. Spivak, *A Comprehensive Introduction to Differential Geometry* (Publish or Perish, Inc., Berkeley, 1979), Vol. 3, Chap. 4.